

# The Aryl Hydrocarbon Receptor and Aryl Hydrocarbon Receptor Nuclear Translocator Protein Show Distinct Subcellular Localizations in Hepa 1c1c7 Cells by Immunofluorescence Microscopy

RICHARD S. POLLENZ,<sup>1</sup> CAROL A. SATTler, and ALAN POLAND

McArdle Laboratory for Cancer Research, University of Wisconsin, Madison, Wisconsin 53706

Received September 21, 1993; Accepted December 21, 1993

## SUMMARY

The aryl hydrocarbon receptor (AhR) and AhR nuclear translocator (Arnt) protein were evaluated in the Hepa 1c1c7 (Hepa-1) cell line by indirect immunofluorescence microscopy and Western blot analysis. Wild-type (WT) Hepa-1 cells stained for AhR show intense cytoplasmic fluorescence with minimal nuclear reactivity. WT cells treated with 2,3,7,8-tetrachlorodibenzo-*p*-dioxin (TCDD) show a time-dependent decrease in cytoplasmic AhR staining and a concomitant increase in nuclear fluorescence. WT cells stained for Arnt show nuclear fluorescence with minimal cytoplasmic reactivity, a pattern unchanged after TCDD treatment. Hepa-1 type II variants express normal levels of AhR but are defective in TCDD-mediated induction of cytochrome P4501A1. Type II variants stained for Arnt show reduced nuclear fluorescence, compared with WT cells, and express minimal

levels of Arnt protein, as determined by Western blot analysis. Type II variants stained for the AhR show intense cytoplasmic fluorescence that becomes nuclear after TCDD treatment. Detailed evaluation by immunoelectron microscopy of the AhR and Arnt present in the nuclear compartment of WT cells shows that both proteins are uniformly distributed and do not appear to be associated with nuclear pores, membranes, or nucleoli. Western blot analysis of nuclei isolated from WT Hepa-1 cells fractionated with Nonidet P-40 shows that minimal levels of AhR or Arnt are retained in the nuclear fraction after TCDD treatment. Collectively, these results indicate that the unliganded AhR resides in the cytoplasm, Arnt is localized to the nucleus, and Hepa-1 cells defective in Arnt expression exhibit TCDD-mediated nuclear accumulation of the AhR.

Exposure to TCDD and related halogenated aromatic hydrocarbons produces a wide range of biological responses in animals (1, 2). These include the direct transcriptional activation of several enzymes, a wasting syndrome, thymic atrophy, epithelial proliferation, teratogenicity, and tumor promotion. At present, the events that ultimately cause many of these responses are poorly understood; however, the process requires binding of an agonist to a soluble protein termed the AhR and transcriptional activation of specific genes (2, 3).

The AhR has been identified in nearly all vertebrates ex-

amined and is expressed in a wide range of tissues (4-6). The unliganded AhR is found in the high-speed supernatant fraction of tissue homogenates as a high molecular mass complex of 280 kDa (9 S) (7, 8) that contains hsp90 (9-11). Recent studies suggest that hsp90 is required to maintain the ligand-free receptor in a high affinity binding conformation (11). After ligand binding, a fraction of the AhR can be isolated by salt extraction of "nuclear" pellets, but the complex is smaller (176 kDa, 6 S) and does not contain hsp90 (7-12). *In vitro* and *in vivo* the 6-S but not the 9-S complex binds specific DNA enhancer sequences termed DREs (13-16). Recently, it has been shown that the transcriptionally active 6-S complex is a heterodimer of the ligand-bound AhR and a protein termed Arnt (17-21). The Arnt protein was named for its suggested role in the nuclear translocation of the liganded AhR (17). From the deduced amino acid sequences of the cDNAs for the

This work was supported in part by grants to A.P. from the National Institute of Environmental Health Sciences (Grant ES01884) and the National Cancer Institute (Grant 07175) and a fellowship to R.S.P. from the National Institute of Environmental Health Sciences (Fellowship F2E505615A).

<sup>1</sup> Current address: School of Pharmacy, University of Wisconsin, 425 N. Charter St., Madison WI 53706.

**ABBREVIATIONS:** TCDD, tetrachlorodibenzo-*p*-dioxin; DMSO, dimethylsulfoxide; DMEM, Dulbecco's modified Eagle medium; PBS, phosphate-buffered saline; SDS, sodium dodecyl sulfate; PAGE, polyacrylamide gel electrophoresis; FBS, fetal bovine serum; DRE, dioxin-responsive element; AhR, aryl hydrocarbon receptor; Arnt, aryl hydrocarbon receptor nuclear translocator; bHLH, basic helix-loop-helix; BEAR, bacterially expressed aryl hydrocarbon receptor; BEARNT, bacterially expressed aryl hydrocarbon receptor nuclear translocator; GAR-TR, goat anti-rabbit IgG conjugated to Texas Red; GAR-G, goat anti-rabbit IgG conjugated to 6-nm gold; GAR-AP, goat anti-rabbit IgG conjugated to alkaline phosphatase; WT, wild-type; hsp90, 90-kDa heat shock protein; Hepa-1, Hepa 1c1c7; HEPES, 4-(2-hydroxyethyl)-1-piperazineethanesulfonic acid; MOPS, 3-(*N*-morpholino)propanesulfonic acid; EGTA, ethylene glycol bis( $\beta$ -aminoethyl ether)-*N,N,N',N'*-tetraacetic acid.

AhR and Arnt proteins, it has been shown that both proteins contain a bHLH region, which is a motif shared by a number of dimeric transcription factors (18, 22–24).

The murine hepatoma cell line Hepa-1 has become an important model system to study the AhR-, Arnt-, and TCDD-mediated induction of *CYP1A1* (cytochrome P4501A1) (25, 26). Hepa-1 cell lines defective in the induction of *CYP1A1* have been selected after mutagenesis, and they fall into distinct complementation groups (27–29). One class (group A variants) contains defects in cytochrome P4501A1. Type I (group B)<sup>2</sup> variants express a reduced number of AhRs that appear to bind TCDD normally and can be isolated from nuclei after [<sup>3</sup>H] TCDD treatment. Type II (group C) variants contain WT levels of AhR and bind TCDD normally, but the AhR cannot be isolated from nuclei after [<sup>3</sup>H] TCDD treatment. TCDD-mediated induction of *CYP1A1* can be partially rescued in group C cells by transfection of human Arnt cDNAs (18). The defect in type II cells is undefined but presumably involves Arnt.

At present, there is little information concerning the subcellular distribution of the AhR or Arnt proteins and their response to agonists *in vivo*. Most of the studies concerning the AhR and Arnt proteins have used disrupted cell and tissue fractions or *in vitro* transcription-translation systems. In this report, we describe the production and characterization of specific polyclonal antibodies to the AhR and Arnt proteins. We use the antibodies to evaluate the subcellular distribution of AhR and Arnt in the various Hepa-1 cell lines by indirect immunofluorescence microscopy, electron microscopy, and Western blot analysis. The results show that 1) the unliganded AhR resides in the cytoplasm in all Hepa-1 cell lines, 2) a significant fraction of the AhR becomes translocated to the nucleus after ligand binding in WT Hepa-1 cells, type II variants, and group C variants, 3) the Arnt protein resides in the nucleus in all Hepa-1 cell lines, and 4) subcellular fractionation methods do not accurately preserve the distribution of the AhR and Arnt observed *in vivo*.

## Experimental Procedures

**Materials.** TCDD was a gift from Dow Chemical Co., 2,7-dichlorodibenzo-*p*-dioxin was a gift from Dr. David Firestone (Food and Drug Administration), 2,3,2',3'-tetrachlorobiphenyl was purchased from Analabs Inc. (North Haven, CT), and 3,4,3',4'-tetrachlorobiphenyl was purchased from RFR Corp. (Hope, RI); 2,4,5,2',4',5'-hexabromobiphenyl and 3,4,5,3',4',5'-hexabromobiphenyl were synthesized by Dr. Andrew Kende, University of Rochester. All compounds were solubilized in DMSO.

**Buffers.** MENG is 25 mM MOPS, pH 7.5, 1 mM EDTA, 0.02% sodium azide, 10% glycerol. PBS is 0.8% NaCl, 0.02% KCl, 0.14% Na<sub>2</sub>HPO<sub>4</sub>, 0.02% KH<sub>2</sub>PO<sub>4</sub>, pH 7.4. The 2× sample buffer is 125 mM Tris, pH 6.8, 4% lithium dodecyl sulfate, 25% glycerol, 4 mM EDTA, 20 mM dithiothreitol, 0.005% bromophenol blue. TTBS is 50 mM Tris, 0.2% Tween 20, 150 mM NaCl, pH 7.5. TTBS+ is 50 mM Tris, 0.5% Tween 20, 300 mM NaCl, pH 7.5. BLOTTO is 5% dry milk in TTBS. Blocking buffer is PBS containing 4% bovine serum albumin.

### Construction of bacterial expression vectors and purification

of fusion protein. The base plasmid used in all constructs was pQE (Qiagen, Chatsworth, CA), which permits inducible expression of proteins fused to six histidine residues at either the amino or carboxyl terminus. For the AhR, the 1400-base pair *AseI*-*Bam*HI restriction fragment (corresponding to amino acids 61–419) was cut from the mouse *Ah*<sup>b-1</sup> allele cDNA (24) and blunt-end ligated into vector pQE8 at the *Bam*HI site, to generate pBEAR-1. This plasmid expressed the BEAR-1 protein, which migrated on SDS-PAGE at approximately 40 kDa. For Arnt, a 1365-base pair fragment of the Arnt open reading frame (amino acids 318–773, based on the human cDNA sequence) (18) was isolated after polymerase chain reaction of mouse mRNA. The purified fragment was ligated into pQE12 to generate pBEARNT. This plasmid expressed the BEARNT protein, which migrated at approximately 50 kDa on SDS-PAGE.

*Escherichia coli* strain M15 cells containing the appropriate plasmid constructs were incubated for 5–6 hr at 37° in the presence of isopropyl-β-D-thiogalactopyranoside (1 mM). Pelleted cells were disrupted by sonication and inclusion bodies were purified by centrifugation. Fusion protein was purified from inclusion bodies under denaturing conditions, as described by the manufacturer (Qiagen). The eluted protein was dialyzed against trifluoroacetic acid (0.1%) and lyophilized. Freeze-dried protein was stored at –20° until use.

**Immunization, bleeding, serum preparation, and storage.** The lyophilized protein (400–500 μg) was suspended in sterile saline solution, emulsified by mixing with an equal volume of Freund's adjuvant, and administered subcutaneously and intramuscularly into New Zealand white rabbits (6). Two or three animals were used for each antigen. The animals were bled 10 days after each booster immunization. After addition of sodium azide, the blood was heated at 37° for 1 hr, chilled at 0° for 1 hr, and centrifuged. The serum was stored at –20° until affinity purification.

**Affinity gel preparation and antibody purification.** The purified fusion protein was solubilized to 2 mg/ml in 0.1 M NaHCO<sub>3</sub>, 0.5 M NaCl, pH 9.0, containing 2% SDS, and was mixed with an equal volume of hydrated cyanogen bromide-activated Sepharose 4B (Sigma Chemical Co., St. Louis, MO) for 3 hr at 22°. The coupling efficiency was generally 50–90%, as determined by analyzing the unbound protein in the supernatant. After blocking with ethanolamine, the resin was extensively washed with the following series of solutions: 1) 1 mg/ml bovine serum albumin in PBS, 2) 25% ethanol in PBS, 3) 50% ethanol in PBS, 4) 25% ethanol in PBS, and 5) PBS. The gel was then resuspended in Tris buffer (10 mM, pH 7.5) containing sodium azide (0.02%). Immune IgG was affinity purified as described (6). Preimmune IgG was isolated from rabbit serum by Protein A-Sepharose chromatography (30).

Affinity-purified antibodies specifically depleted of immune IgG (preabsorbed antibodies) were generated as follows. The purified fusion proteins were separated by SDS-PAGE and blotted to nitrocellulose, and the band migrating at 40 kDa (BEAR-1) or 50 kDa (BEARNT) was excised. The immobilized protein was then incubated with affinity-purified IgG (1–3 μg/ml) in blocking buffer for 24 hr at 4°. The solution was filtered through 0.45-μm filters and stored at 4° until use.

**Nomenclature of antibodies.** Antibodies to the BEAR-1 fusion protein that react specifically with the AhR are termed A-1. Antibodies to the BEARNT fusion protein that react specifically with Arnt are termed R-1. These antibodies were used as the affinity-purified IgG fraction, unless otherwise noted. GAR-TR, GAR-G, and GAR-AP were purchased from Jackson ImmunoResearch (West Grove, PA). The concentrations of the antibodies used in each experiment are indicated in the text.

**Cells and growth conditions.** WT Hepa-1 cells, type I variants, and type II variants were a generous gift from Dr. Jim Whitlock, Jr. (Department of Pharmacology, Stanford University). The cells were propagated in DMEM containing 5% FBS. Dr. Oliver Hankinson (Department of Environmental Medicine, University of California, Los Angeles) generously provided group B (B15ECiii20 u<sup>R</sup>TG<sup>4</sup>) and group C (B13NBii1TG<sup>4</sup>) Hepa-1 variants. These cells were propagated in

<sup>2</sup> Type I and type II variants were isolated by Dr. J. Whitlock. Group A, B, and C variants were isolated by Dr. O. Hankinson. There are presently no reports that directly compare the different variants from the independent laboratories. Because type I and group B cells and type II and group C cells exhibit similar phenotypes, we assume (for this study) that they belong to the same complementation groups. Both sets of cells were evaluated in the experiments described in this report, although most of the data presented are derived from the cells obtained from Dr. Whitlock.

$\alpha$ -modified Eagle medium containing 5% FBS. In some experiments, cells were propagated in DMEM containing adsorbed FBS or in DMEM that did not contain phenol red. FBS was adsorbed with 1% charcoal/0.1% dextran for 30 min at room temperature, centrifuged at 3000 rpm, and then sterilely filtered.

**Cell growth and fixation.** Cells were detached from growth flasks by trypsinization (0.05% trypsin/0.5 mM EDTA), centrifuged, and resuspended in appropriate growth medium at a density of  $2-5 \times 10^5$ /ml. Cells were pipetted into culture dishes containing sterile glass coverslips coated with poly-L-lysine (0.01%; Sigma) or onto Permanox chamber slides (Lab Tech, Naperville, IL). Cells were propagated in appropriate medium for 1–4 days at 37°, washed extensively with PBS, and incubated with vehicle (DMSO) or test compound in DMEM without FBS, for the times indicated in the text.

Subconfluent cells on coverslips were washed with PBS at 22° and then fixed for 30 min at room temperature in PBS containing 4% paraformaldehyde, pH 7.4. Coverslips were washed in PBS (2–3 min), dried by aspiration, and immersed in 100% anhydrous methanol at –20° for 4 min. Coverslips were removed, allowed to dry, rinsed twice in PBS, and then stored at 4° in PBS containing 0.02% sodium azide. Cells were stained within 2 weeks of fixation. To verify morphology, cells were stained with hematoxylin and eosin as described (30).

**Immunofluorescence staining and microscopy.** Coverslips were incubated in blocking buffer (22°) for 2 hr, followed by fresh blocking buffer containing appropriate primary antibody for 1–3 hr (22°). The primary antibodies in blocking buffer were filtered through a 0.45- $\mu$ m filter and used at 1–3  $\mu$ g/ml. Coverslips were rinsed with PBS and washed with three changes of TTBS+ for a total of 45 min. The washed coverslips were rinsed with PBS and incubated for 1 hr at 22° in PBS containing GAR-TR (1/750 dilution). The final secondary antibody solution was filtered before use as described above. Coverslips were washed in TTBS+ as described above, rinsed extensively with distilled water to remove all salt and detergent, and mounted onto glass slides in 50% glycerol containing 2% *n*-propyl galate (Sigma). Once dry, coverslips were sealed to slides with nail polish.

Fluorescence was observed with a Zeiss Axiophot microscope, using the 568-nm filter. On average, 15–20 fields (5–20 cells each) were evaluated on each slip, and three were photographed to generate the raw data. Experiments were repeated at least three times. The intensity of fluorescence varied between experiments but the pattern of staining was always consistent. All cells were photographed and printed with constant exposure times.

**Electron microscopy.** Cells were propagated on Permanox chamber slides and fixed with paraformaldehyde as described above. Cells were incubated in blocking buffer for 1–2 hr at 22° and then incubated with primary antibody (3  $\mu$ g/ml) in blocking buffer for 16–24 hr at 4°. Chamber slides were rinsed with PBS and washed for 1 hr with four changes of TTBS+. Slides were then incubated for 16–24 hr at 4° with GAR-G (1/15 dilution) in PBS containing 5% normal goat serum. Slides were washed in TTBS+ as described above and then fixed for 15 min with 1% glutaraldehyde in 0.1 M cacodylate buffer, pH 7.4. Slides were washed in buffer and postfixed with 2% osmium tetroxide for 30 min. The slides were then washed with distilled water, dehydrated in a graded series of alcohols, and infiltrated in a mixture of propylene oxide and Eponate (Ted Pella, Redding, CA). After infiltration, each Permanox slide was inverted on a slide-duplicating mold (Electron Microscopy Sciences, Fort Washington, PA), filled with Eponate, and polymerized at 60° for 36 hr. The monolayer was immersed in liquid nitrogen to separate it from the slide. Small areas of the monolayer were cut out with a jeweler's saw and glued onto an epoxy stub. Monolayers were sectioned on a Reichert Ultracut E3 microtome equipped with a diamond knife. Thin sections were examined unstained or stained in an Hitachi H-7000 electron microscope operated at 75 kV.

**Preparation of cell cytosol.** Cytosol was prepared by two methods. In method 1, Hepa-1 cells were detached from growth flasks by trypsinization (0.05% trypsin/0.5 mM EDTA), washed twice with PBS, and

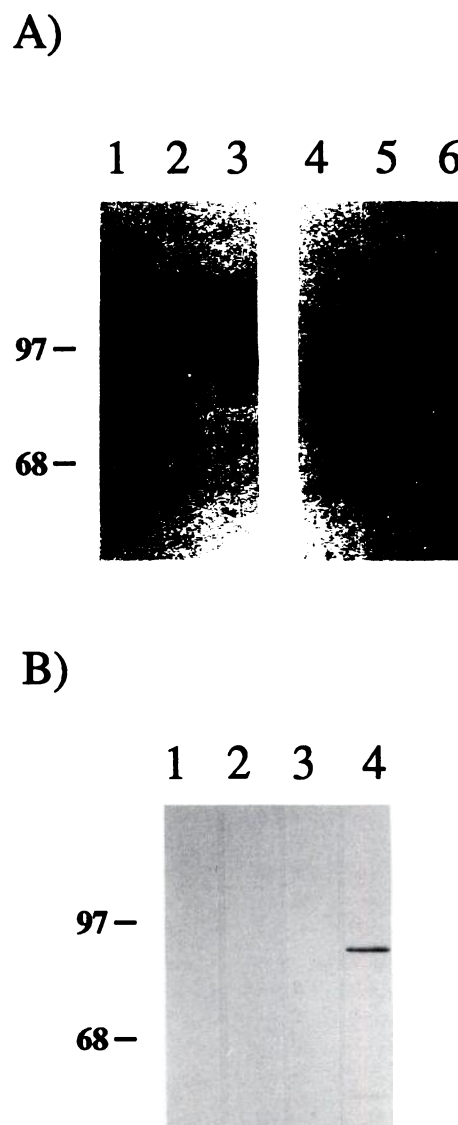


**Fig. 1.** Western blot analysis of Hepa-1 cytosol. One hundred micrograms of cytosol were resolved on 7.5% SDS-PAGE gels, transferred to nitrocellulose, and incubated with A-1 (2  $\mu$ g/ml), R-1 (2  $\mu$ g/ml), preabsorbed A-1, preabsorbed R-1, or preimmune rabbit IgG (2  $\mu$ g/ml). Antibody binding was visualized by staining of the blots with GAR-AP, as detailed in Experimental Procedures. **A,** Lane 1, WT Hepa-1 cytosol stained with A-1; lane 2, type I Hepa-1 cytosol stained with A-1; lane 3, type II Hepa-1 cytosol stained with A-1; lane 4, WT Hepa-1 cytosol stained with R-1; lane 5, type I Hepa-1 cytosol stained with R-1; lane 6, type II Hepa-1 cytosol stained with R-1. **B,** Lane 1, WT Hepa-1 cytosol stained with preabsorbed A-1; lane 2, WT Hepa-1 cytosol stained with preabsorbed R-1; lane 3, WT Hepa-1 cytosol stained with preimmune IgG; lane 4, 20  $\mu$ g of WT Hepa-1 cytosol stained with 1  $\mu$ g/ml A-1 as control.

centrifuged at 1000 rpm. Trypsinization was utilized so that cells could be accurately counted and processed in small volumes of buffer. Cell pellets were suspended to  $1 \times 10^8$ /ml in MENG supplemented with molybdate (20 mM), EDTA (5 mM), and 2-mercaptoethanol (10 mM), at 4°. Cells were homogenized with 50 strokes in a Dounce homogenizer and centrifuged at  $100,000 \times g$  for 1 hr at 4°. In method 2, cells were harvested and washed as described above. Cells were suspended in 1 volume of 2 $\times$  lysis buffer (50 mM HEPES, pH 7.4, 2 mM dithiothreitol, 40 mM sodium molybdate, 10 mM EGTA, 6 mM  $MgCl_2$ , 20% glycerol, 0.1 mg/ml phenylmethylsulfonyl fluoride) supplemented with 2% Nonidet P-40 and were gently triturated. Suspensions were centrifuged at 1000 rpm and the supernatant was removed. Pellets (nuclei) were

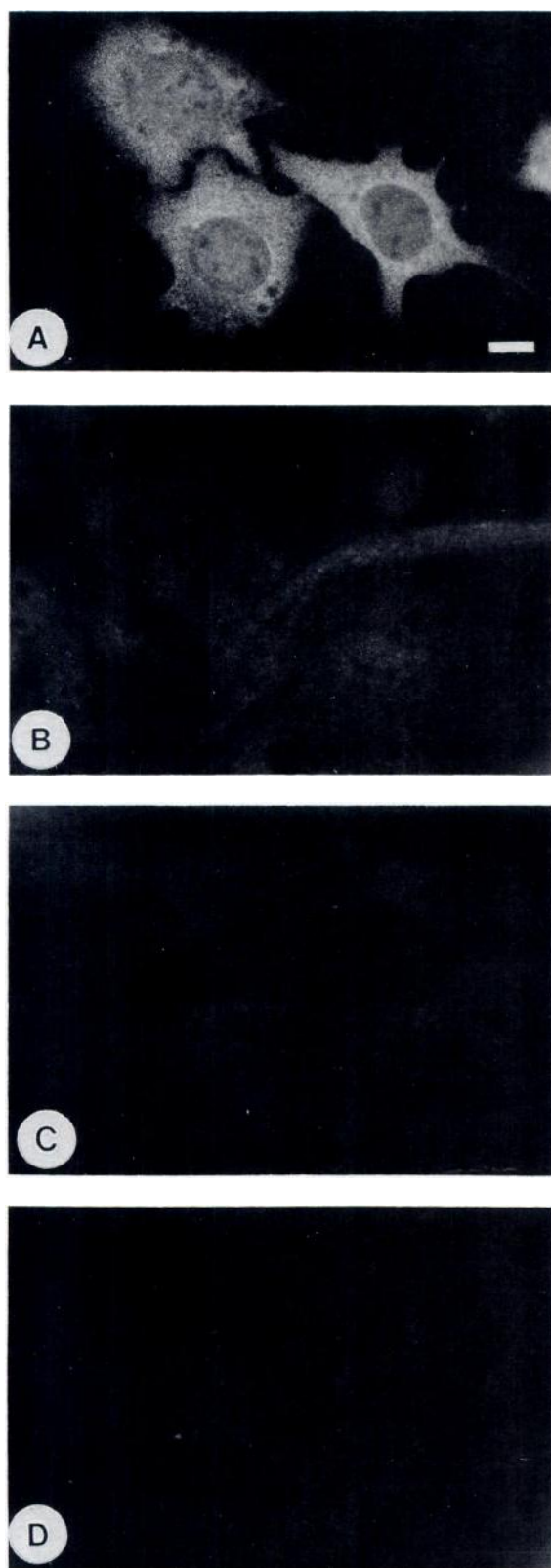


**Fig. 2.** Immunofluorescence microscopy of Hepa-1 cells stained for the AhR. All cells were propagated in DMEM/5% FBS, fixed, and stained with 1  $\mu$ g/ml A-1 and GAR-TR (1/750) unless otherwise noted. A, WT Hepa-1 cells; B, type I Hepa-1 cells; C, WT Hepa-1 cells stained with preabsorbed A-1 and GAR-TR (1/750); D, WT Hepa-1 cells stained with preimmune IgG (1  $\mu$ g/ml) and GAR-TR (1/750). Bar, 10  $\mu$ m.

washed twice with 1 $\times$  lysis buffer and suspended to the same volume as the cytosol with 1 $\times$  lysis buffer. Nuclei were uniform in appearance and no intact cells were observed by light microscopy. Nuclei were briefly digested with DNase (0.02 mg/ml) for 5 min at 4 $^{\circ}$  and then sonicated for 30 sec. All samples were stored at -80 $^{\circ}$  until use.

**SDS-PAGE and Western blotting.** Protein samples were resolved by denaturing SDS-PAGE on discontinuous polyacrylamide slab gels and were electrophoretically transferred to nitrocellulose or polyvinylidene difluoride membranes (Millipore) as described (6). The blot was incubated with 0.1% Ponceau S (in 1% acetic acid) to visualize protein bands, washed in distilled water, and incubated in BLOTTO buffer for 1-2 hr at 22 $^{\circ}$ . Blots were then washed in TTBS, dried, and stored in cellophane at 4 $^{\circ}$ . Immunochemical staining was carried out for 1-2 hr at 22 $^{\circ}$  with varying concentrations of primary antibody in BLOTTO buffer. Blots were washed with three changes of TTBS+ for a total of 45 min. The blots were then incubated for 1 hr at 22 $^{\circ}$  in BLOTTO buffer containing a 1/5000 dilution of GAR-AP and were washed with three changes of TTBS+ as described above. Color development was performed with nitro blue tetrazolium/5-bromo-4-chloro-3-indolyl phosphate as a reagent (30).

## Results

**The A-1 and R-1 antibodies show high specificity for Hepa-1 cell cytosol.** The specificity of the R-1 and A-1 antibodies was determined by immunochemical staining of Western blots of cytosolic fractions prepared from WT, type I, and type II Hepa-1 cells. Previous reports indicated that Hepa-1 cells express the *Ah*<sup>b-1</sup> allele of the AhR, which has a molecular mass of approximately 95 kDa (6, 24). The molecular mass of human Arnt is approximately 87 kDa (18, 19). Fig. 1A shows two identical blots, stained with either the A-1 or R-1 antibody.

The A-1 antibody reacts predominantly with a protein of approximately 95 kDa in WT and type II cytosol (Fig. 1A, lanes 1 and 3) and shows reduced immunoreactivity with type I cytosol (Fig. 1A, lane 2). WT Hepa-1 cytosol stained with preabsorbed A-1 or preimmune IgG (Fig. 1B, lanes 2 and 3, respectively) shows minimal immunoreactivity. To confirm that the A-1 antibody reacts with authentic AhR, WT Hepa-1 cytosol was photoaffinity labeled with 2-azido-3-[<sup>125</sup>I]iodo-7,8-dibromodibenzo-*p*-dioxin, as described previously (31). The protein recognized by A-1 is specifically labeled in these experiments (data not shown).

The R-1 antibody primarily stains a protein that migrates slightly faster than the AhR in both WT and type I cytosol (Fig. 1A, lanes 4 and 5). The cytosol from type II cells shows reduced immunoreactivity (Fig. 1A, lane 6), consistent with the idea that these cells have a defect in Arnt. WT Hepa-1 cytosol stained with preabsorbed R-1 also shows minimal immunoreactivity (Fig. 1B, lane 4). Further confirmation of R-1 specificity is its ability to precipitate the AhR-Arnt heterodimer from TCDD-treated cytosol and to produce a "supershift" when included in gel-shift assays with nuclear extracts of TCDD-treated WT Hepa-1 cells (20).<sup>3</sup>

**The unliganded AhR is localized to the cytoplasm in WT Hepa-1 cells.** WT Hepa-1 cells fixed and then stained with the A-1 antibody show intense punctate fluorescence throughout the cytoplasm and exhibit minimal nuclear staining

<sup>3</sup> Richard S. Pollenz, unpublished observations.



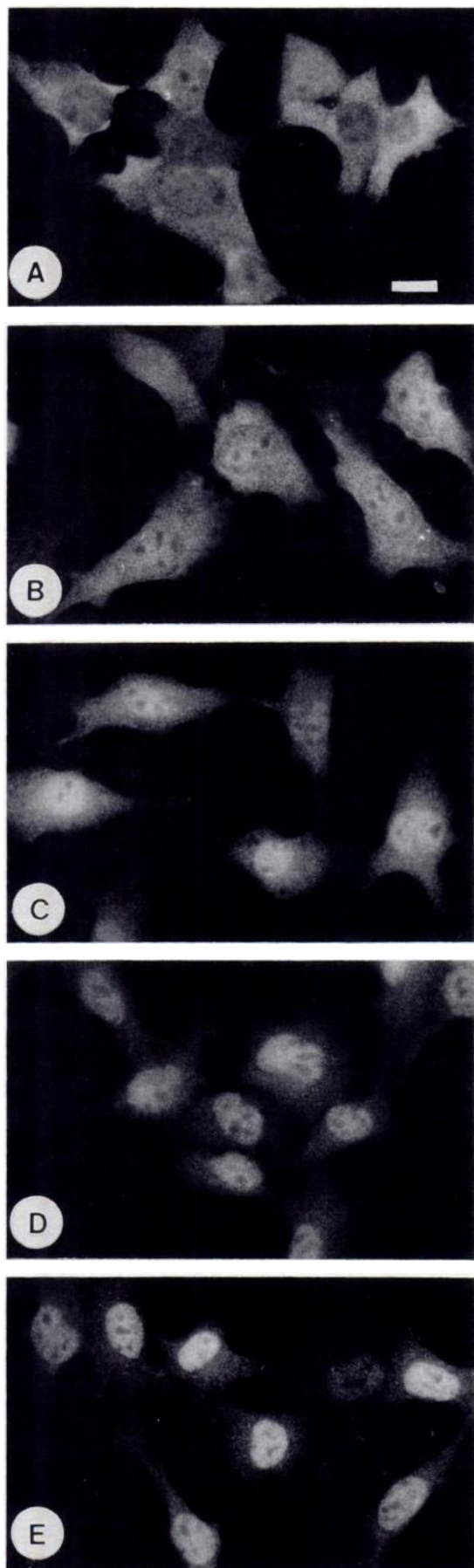


(Fig. 2A).<sup>4</sup> Type I cells stained under identical conditions exhibit markedly diminished cytoplasmic fluorescence, consistent with their reduced expression of the AhR (Fig. 2B). Group B cells stained with A-1 also show a significant decrease in cytoplasmic fluorescence (data not shown). To confirm that the cytoplasmic staining is specific for the A-1 antibody, WT Hepa-1 cells were stained with preabsorbed A-1 (Fig. 2C) or preimmune IgG (Fig. 2D). Cells stained under these conditions show minimal fluorescence.

**The AhR shows a dramatic redistribution to the nucleus in WT Hepa-1 cells treated with agonists.** WT Hepa-1 cells were treated with various AhR agonists, fixed, and then stained with the A-1 antibody. Cells fixed immediately after treatment with 2 nM TCDD (time 0) exhibit intense punctate fluorescence primarily in the cytoplasm (Fig. 3A). With increasing duration of TCDD exposure, there is a progressive decrease in the cytoplasmic fluorescence and a concomitant increase in nuclear fluorescence (Fig. 3, B-E). After 120 min of TCDD treatment (Fig. 3E), the nucleus shows an intense uniform pattern of fluorescence, whereas the cytoplasmic staining approaches the background level observed in cells stained with preimmune IgG (see Fig. 2D). When WT Hepa-1 cells are treated with other agonists such as 3,4,5,3',4',5'-hexabromobiphenyl or 3,4,3',4'-tetrachlorobiphenyl (Fig. 4, A and B, respectively), the A-1 staining is also localized to the nucleus and cytoplasmic fluorescence is diminished. WT Hepa-1 cells treated with inactive congeners such as 2,4,5,2',4',5'-hexabromobiphenyl, 2,3,2',3'-tetrachlorobiphenyl, or 2,7-dichlorobiphenyl (Fig. 4, C, D, and E, respectively) exhibit punctate cytoplasmic fluorescence and minimal nuclear staining. These compounds do not induce P4501A1 activity in structure-activity studies (32). In addition, when WT Hepa-1 cells are treated with TCDD for 90 min at 4°, the A-1 staining remains cytoplasmic (Fig. 4F; compare with DMSO-treated cells in Fig. 4G and TCDD-treated cells at 37° in Fig. 4H).

**Arnt is localized to the nucleus in WT Hepa-1 cells.** WT Hepa-1 cells fixed and then stained with the R-1 antibody show intense nuclear fluorescence and minimal cytoplasmic fluorescence (Fig. 5A). The nuclear fluorescence appears uniform, is excluded from nucleolar regions, and does not appear to be concentrated at nuclear membranes. Type II cells stained with R-1 show a significant decrease in the level of nuclear fluorescence, compared with WT Hepa-1 cells, but generally exhibit a similar level of cytoplasmic staining (Fig. 5D). Similar results are observed when group C cells are stained with R-1.<sup>5</sup> WT Hepa-1 cells stained with preabsorbed R-1 also show markedly reduced nuclear fluorescence (Fig. 5E). WT Hepa-1 cells stained with preimmune IgG exhibit a low level of cyto-

**Fig. 3.** Immunofluorescence microscopy of WT Hepa-1 cells after treatment with TCDD and staining for the AhR. WT Hepa-1 cells were incubated at 37° with TCDD (2 nM) for the indicated intervals, fixed, and then stained with A-1 (1 µg/ml) and GAR-TR (1/750). A, 0 min; B, 15 min; C, 30 min; D, 60 min; E, 120 min. Bar, 10 µm.

<sup>4</sup> The description of fluorescence levels is objective and based on the observation of >1000 untreated WT Hepa-1 cells. In every intact cell, the majority of fluorescence was always present in the cytoplasm, although varying levels of reactivity could be observed in the nuclear compartment. Because the level of nuclear reactivity was always very low, it was not possible to clearly determine its significance. It should be noted that the photographs represent two-dimensional images of three-dimensional structures and that the volume ratio of cytoplasm to nucleus is approximately 9:1. We do not discount the possibility that a small number of AhRs are present in the nuclear compartment.

<sup>5</sup> Richard S. Pollenz, unpublished observations.

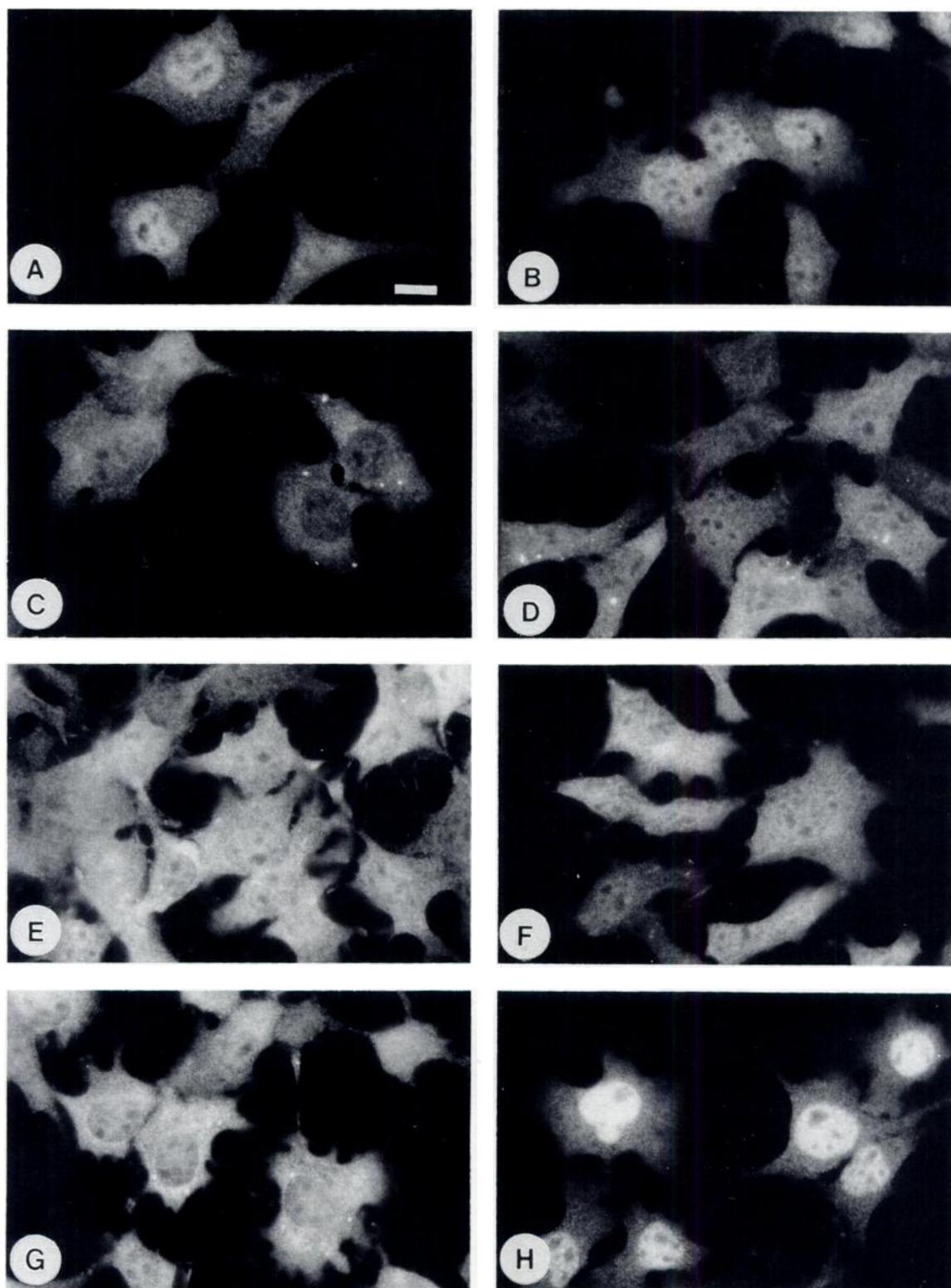


**Fig. 4.** Immunofluorescence microscopy of WT Hepa-1 cells after staining for the AhR after different treatments. WT Hepa-1 cells were treated for 90 min at 37° (unless otherwise noted), fixed, and stained with A-1 (1  $\mu$ g/ml) and GAR-TR (1/750). A, 250 nM 3,4,5,3',4',5'-hexabromobiphenyl treatment; B, 250 nM 3,4,3',4'-tetrachlorobiphenyl; C, 250 nM 2,4,5,2',4',5-hexabromobiphenyl; D, 250 nM 2,3,2',3'-tetrachlorobiphenyl; E, 10 nM 2,7-dichlorodibenzo-*p*-dioxin; F, 2 nM TCDD for 90 min at 4°; G, vehicle control (0.1% DMSO); H, 2 nM TCDD for 90 min at 37°. Bar, 10  $\mu$ m.

plasmic fluorescence, which is similar to that observed in cells stained with R-1 (Fig. 5F).

Previous studies suggest that the glucocorticoid receptor redistributes from the cytoplasm to the nucleus when cultured

cells are incubated with FBS or when phenol red is included in the medium (33). To investigate these findings with respect to the location of Arnt, WT Hepa-1 cells were stained with R-1 after growth in modified DMEM. The nuclear staining is not



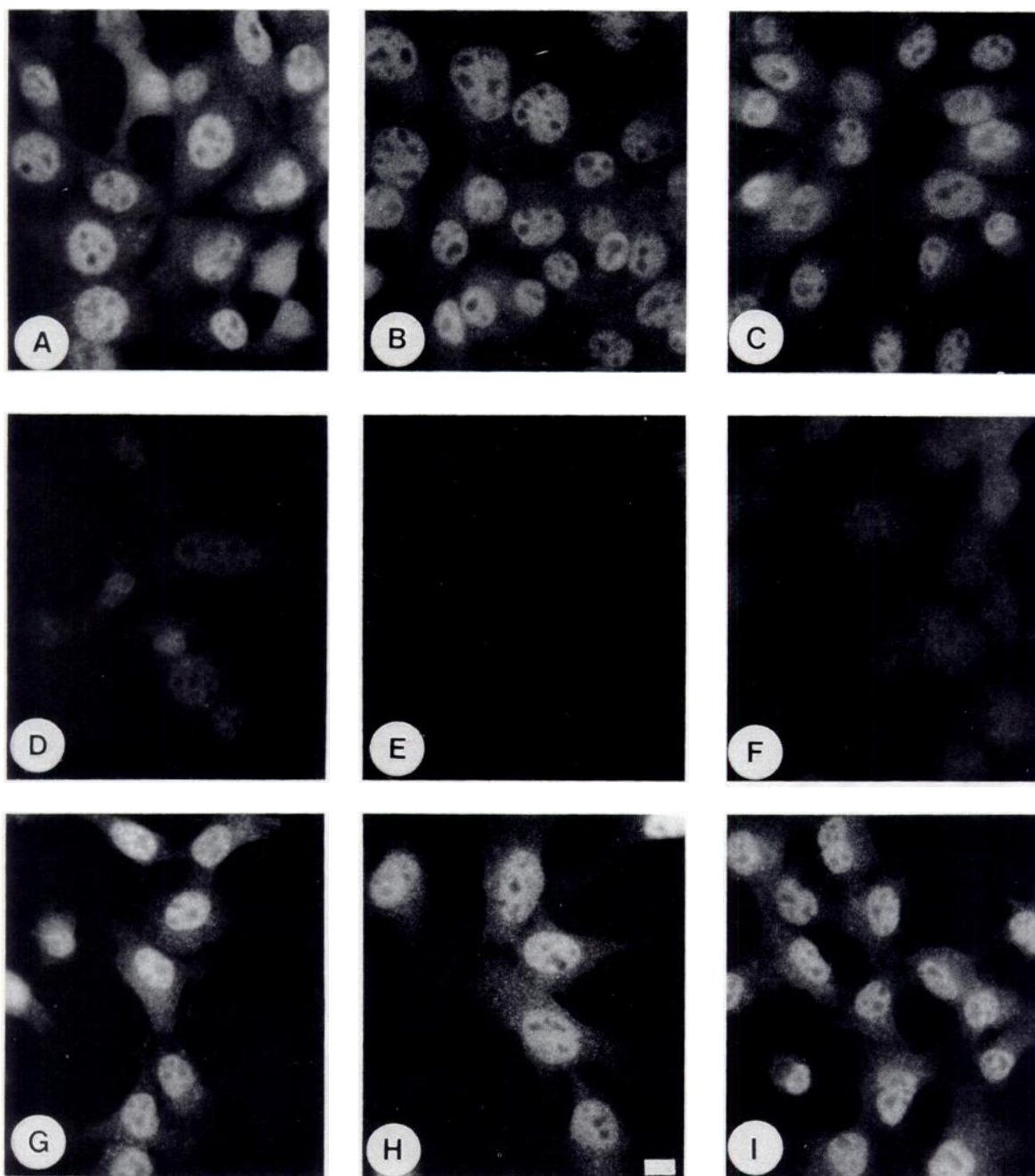


**Fig. 5.** Immunofluorescence microscopy of WT Hepa-1 cells stained for Arnt. WT Hepa-1 cells were propagated in DMEM/5% FBS (or as noted), fixed, and stained with 3  $\mu$ g/ml R-1 and GAR-TR (1/750). A, WT Hepa-1 cells; B, WT Hepa-1 cells grown in DMEM/5% absorbed FBS; C, WT Hepa-1 cells grown in DMEM/5% absorbed FBS without phenol red; D, type II Hepa-1 cells; E, WT Hepa-1 cells stained with preabsorbed R-1 and GAR-TR (1/750); F, WT Hepa-1 cells stained with preimmune IgG (3  $\mu$ g/ml) and GAR-TR (1/750); G, WT Hepa-1 cells treated with 2 nM TCDD for 90 min at 37°; H, WT Hepa-1 cells treated with 250 nM 3,4,5,3',4',5'-hexabromobiphenyl for 90 min at 37°; I, WT Hepa-1 cells treated with 250 nM 3,4,3',4'-tetrachlorobiphenyl for 90 min at 37°. Bar, 10  $\mu$ m.

diminished when cells are grown in medium supplemented with charcoal-absorbed FBS either in the presence or in the absence of phenol red (Fig. 5, B and C, respectively). The R-1 staining also remains nuclear when Hepa-1 cells are propagated for 2 hr in the absence of FBS (data not shown). To investigate the influence of various AhR agonists on the distribution of Arnt, WT Hepa-1 cells were incubated with TCDD, 3,4,5,3',4',5'-hexabromobiphenyl, or 3,4,3',4'-tetrachlorobiphenyl (Fig. 5, G, H, and I, respectively) and stained with R-1. These treatments do not influence the distribution or intensity of the nuclear fluorescence.

**The AhR translocates to the nucleus in type II and group C cells after TCDD treatment.** Previous reports indicated that, after [ $^3$ H]TCDD treatment of type II or group C Hepa-1 cells, the AhR is not recovered in nuclear fractions as it is in [ $^3$ H]TCDD-treated WT Hepa-1 cells (27–29). To investigate these observations, type II and group C cells were treated with TCDD, fixed, and then stained with A-1 as described in Experimental Procedures. At time 0 (Fig. 6A), type II cells exhibit punctate fluorescence primarily in the cytoplasm. After TCDD treatment, the cytoplasmic fluorescence decreases in a time-dependent manner and the nuclei of the

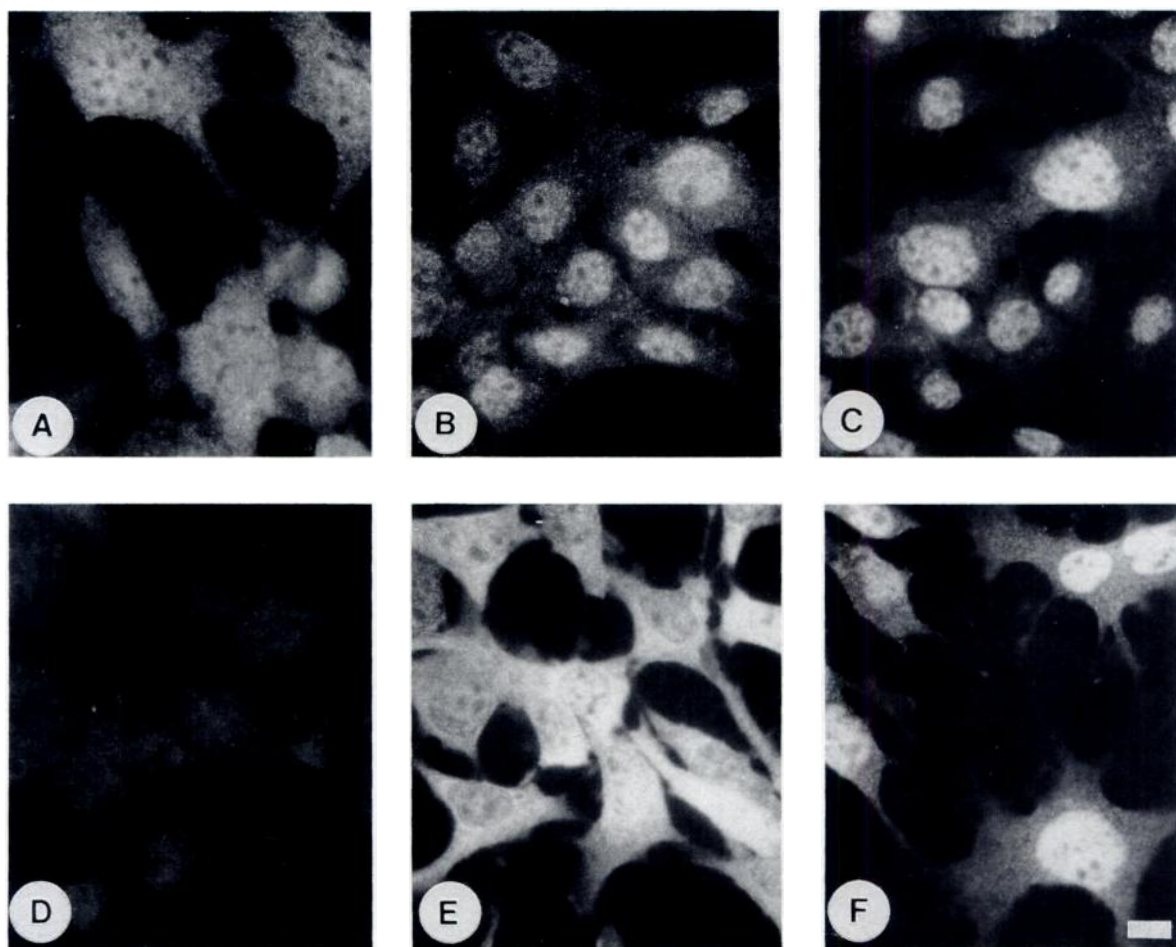


**Fig. 6.** Immunofluorescence microscopy of type II and group C Hepa-1 cells after treatment with TCDD and staining for the AhR. Cells were incubated at 37° with TCDD (2 nM) for the indicated intervals, fixed, and then stained with A-1 (1  $\mu$ g/ml) and GAR-TR (1/750), unless otherwise noted. A-D, Type II variants; E and F, group C variants. A, 0 min; B, 30 min; C, 60 min; D, stained with preimmune IgG (1  $\mu$ g/ml); E, 0 min; F, 60 min. Bar, 10  $\mu$ m.

cells show a concomitant increase in fluorescence (Fig. 6, B and C). One hour after TCDD treatment (Fig. 6C), the staining pattern approximates that observed in WT Hepa-1 cells treated with TCDD (compare with Fig. 4E). Group C variants also show a dramatic redistribution of the AhR from cytoplasm to the nucleus after TCDD treatment (Fig. 6, E and F).

**Evaluation of AhR and Arnt distribution in WT Hepa-1 cells by electron microscopy.** The distribution of AhR and Arnt in the cytoplasm and nucleus was evaluated further by electron microscopy using immunogold-labeled secondary antibodies. The AhR is primarily localized in the cytoplasm of untreated cells and does not appear to be associated with cytoskeleton, intracellular vesicles, or endoplasmic reticulum (data not shown). After treatment with TCDD, there is a significant increase in gold labeling of the nuclear compartment and a concomitant loss of staining in the cytoplasm. AhR staining is uniform throughout the nucleus but is not associated with membranes, nuclear pores, or nucleolar regions. Arnt staining is predominantly nuclear and does not exhibit significant changes in distribution when cells are treated with TCDD (data not shown). To investigate the association of Arnt with structures known to be involved in nuclear transport (34), nuclear membranes were evaluated at high magnification. Fig. 7 shows a section cut through the nuclear membrane to expose

the nuclear pore complexes (Fig. 7, *arrows*). R-1 does not stain these structures and is not found associated with any of the nuclear membranes.

**The AhR and Arnt distribute into the same subcellular compartments when cells are fractionated.** In view of the electron microscopy and immunofluorescence results, it was pertinent to assess the subcellular distribution of the AhR and Arnt by biochemical fractionation methods. WT and type II Hepa-1 cells were disrupted in buffer containing Nonidet P-40, and cytosol and nuclear fractions were prepared as described in Experimental Procedures. Cytosolic and nuclear fractions equivalent to the same quantity of cells were separated by SDS-PAGE and analyzed by Western blotting.

Fig. 8A shows a Western blot of WT and type II Hepa-1 cell fractions stained for the AhR. In vehicle-treated cells, the majority of the AhR is present in the cytosolic fraction (Fig. 8A, *lanes 1 and 2*). After treatment with TCDD, the relative amount of AhR detected in the cytosol appears unchanged, in comparison with untreated cells, but a small amount of AhR is detected in the WT Hepa-1 nuclei (Fig. 8A, *lanes 3 and 4*). The AhR is not detected in the nuclei of TCDD-treated type II cells (Fig. 8A, *lane 6*). Fig. 8B shows an identical blot stained for Arnt. As observed with the AhR, the majority of Arnt is found in the cytosolic fraction of vehicle-treated WT Hepa-1 cells



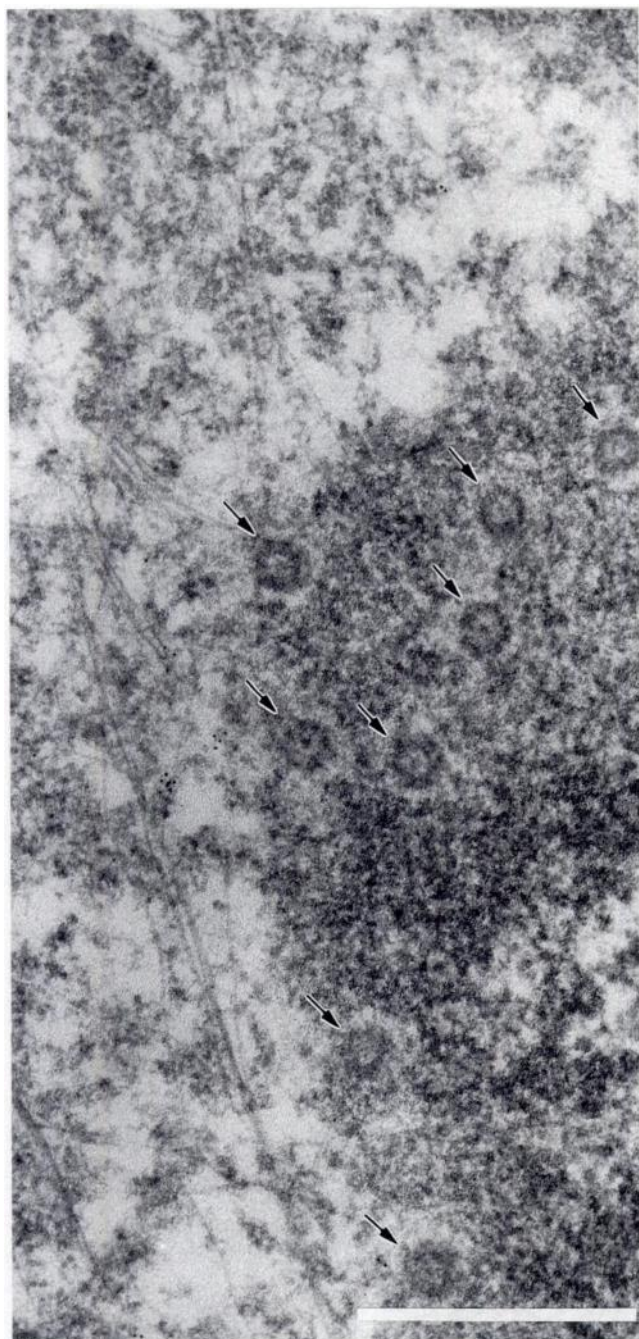


**Fig. 7.** Nuclear pore complexes stained for Arnt. WT Hepa-1 cells were fixed and stained with 3  $\mu\text{g/ml}$  R-1, followed by GAR-G (1/15). Sections were processed for electron microscopy and stained with uranyl acetate as described in Experimental Procedures. Arrows, nuclear pore complexes. Note lack of immunogold staining of these structures and the nuclear membrane. Bar, 0.5  $\mu\text{m}$ .

(Fig. 8B, lanes 1 and 2). When WT Hepa-1 cells are treated with TCDD, the majority of Arnt is detected in the cytosol, but a fraction of the protein is also detected in nuclei (Fig. 8B, lanes 3 and 4). Cytosol and nuclei prepared from type II cells do not exhibit significant Arnt staining (Fig. 8B, lanes 5 and 6).

### Discussion

**The AhR and Arnt reside in distinct subcellular compartments in Hepa-1 cells.** The current model of gene activation by the AhR hypothesizes that the AhR is complexed

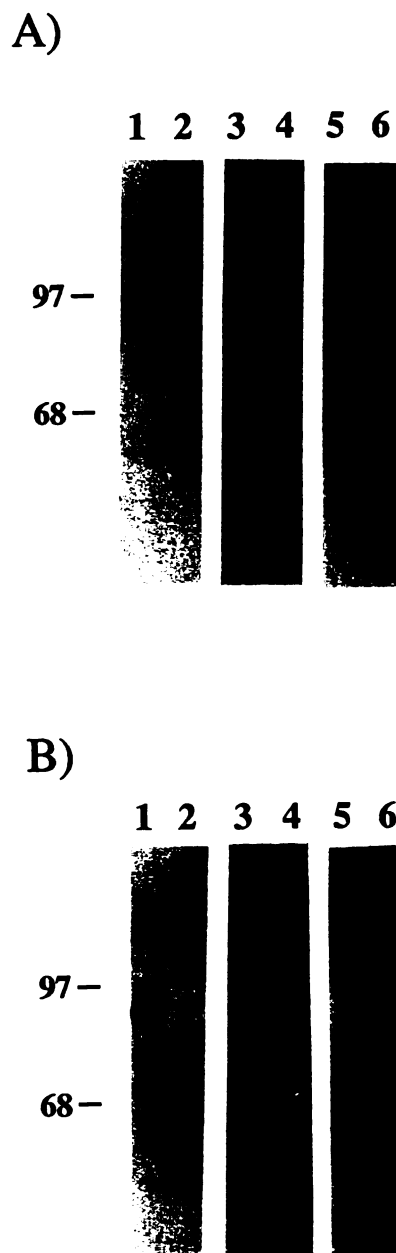


**Fig. 8.** Western blot analysis of WT and type II subcellular fractions. WT and type II cells were treated with vehicle or TCDD (2 nM) for 90 min, and cytosolic and nuclear fractions were prepared. Cytosolic fractions (100  $\mu\text{g}$  of protein) and nuclear fractions (approximately 30  $\mu\text{g}$  of protein) equivalent to the same number of cells were resolved by SDS-PAGE, blotted to nitrocellulose, and stained as described in Experimental Procedures. A, Blot stained with 2  $\mu\text{g/ml}$  A-1. Lane 1, cytosol from vehicle-treated WT cells; lane 2, corresponding nuclei from WT cells; lane 3, cytosol from TCDD-treated WT cells; lane 4, corresponding nuclei from TCDD-treated WT cells; lane 5, cytosol from TCDD-treated type II cells; lane 6, corresponding nuclei from TCDD-treated type II cells. B, Western blot stained with 2  $\mu\text{g/ml}$  R-1. Lanes 1-6, same as in A.

with hsp90 in the cytoplasm, where it binds to an agonist. The AhR then dissociates from hsp90, undergoes a poorly understood activation event, and binds with Arnt, and this ligand-bound heterodimer specifically recognizes the DREs in target genes to regulate transcription (2). These events have been studied largely *in vitro* using disrupted cell fractions; therefore, the subcellular location of the AhR and Arnt *in vivo*, the location of their interaction, and the function of Arnt in nuclear

translocation mechanisms are not known. In this report, we have examined these questions in Hepa-1 cells using affinity-purified polyclonal antibodies specific to the AhR and Arnt. The results show that, in the absence of any added agonist, the AhR is primarily localized in the cytoplasm of Hepa-1 cells, whereas Arnt appears to be localized in the nucleus. Despite the differential localization of the two proteins, a significant fraction of the AhRs appear to translocate to the nucleus after treatment with TCDD, 3,4,5,3',4',5'-hexabromobiphenyl, or 3,4,3',4'-tetrachlorobiphenyl. These agonists do not appear to affect the nuclear localization of the Arnt protein.

The validity of these results is dependent on the specificity of the prepared antibodies and the specificity of the immunofluorescence staining. The A-1 (anti-AhR) and R-1 (anti-Arnt) antibodies used in these experiments are affinity-purified IgG fractions produced against bacterially expressed fusion proteins, and their specificity is supported by a number of experiments. First, the A-1 and R-1 antibodies recognize a single protein species in WT Hepa-1 cell cytosol, as determined by Western blot analysis. Second, the A-1 and R-1 antibodies react poorly with cytosol and whole-cell lysates prepared from type I and type II cells, respectively. These results correlate with the immunofluorescence data, which show that type I cells have reduced AhR staining and type II cells stain poorly for Arnt. Third, both the A-1 and R-1 antibodies can be used to precipitate AhR-Arnt heterodimers from TCDD-treated cytosol, and the antibodies specifically cause supershifts when incubated with AhR-Arnt heterodimers in gel-shift assays.

The finding that Arnt is primarily localized in the nucleus is supported by the finding that the Arnt protein contains an amino acid sequence near its amino terminus that could serve as a nuclear localization signal (Arg-Ala-Ile-Lys-Arg-Pro; amino acids 39–45) (19). Interestingly, the AhR also contains an amino-terminal basic sequence (Arg-Lys-Arg-Arg-Lys-Pro; amino acids 12–17) (23, 24), but it is localized in the cytoplasmic compartment in the unliganded state. The cytoplasmic location of the AhR may be the result of its association with hsp90 (9–11); hsp90 is thought to function in masking the nuclear targeting site or "tethering" the unliganded glucocorticoid receptor in the cytoplasmic compartment (33, 35). It is not known whether Arnt is bound to other proteins in the absence of liganded AhR, but these results suggest that Arnt complexes with the liganded AhR in the nuclear compartment and not the cytoplasm.

**Hepa-1 cell lines defective in Arnt protein exhibit TCDD-mediated nuclear localization of the AhR.** Type II and group C Hepa-1 cell variants are characterized by 1) normal binding of radioligand to the AhR in the cytosolic fraction *in vitro*, 2) failure of AhR agonists to induce cytochrome P450A1, and 3) failure to detect the AhR in the nuclear fraction of disrupted cells after [<sup>3</sup>H]TCDD treatment (27–29). The *arnt* gene was isolated after complementation of the defect in group C cells and partial restoration of TCDD-mediated P450A1 induction and nuclear localization of the AhR (18). It has subsequently been shown that the Arnt protein is a component of the complex that contains the liganded AhR and specifically binds to DREs (19–21). The function of Arnt in nuclear translocation mechanisms has not been formally evaluated.

In this report we have used immunofluorescence microscopy to demonstrate that the AhR accumulates in the nucleus of TCDD-treated type II and group C Hepa-1 cells (which express

minimal levels of Arnt protein), in a manner indistinguishable from that of WT Hepa-1 cells. However, when the nuclear fraction from TCDD-treated type II cells is evaluated by Western blot analysis the AhR is not detected, and the AhR is found in the cytosolic fraction. Similarly, WT Hepa-1 cells treated with TCDD exhibit intense AhR and Arnt staining in the nucleus by immunofluorescence, but upon cell fractionation and Western blot analysis only a small fraction of total AhR and Arnt is detected in the nucleus. These results suggest that the majority of AhR and Arnt redistribute from the nuclei during fractionation. This explanation is supported by the observation that we detect the 200-kDa subunit of RNA polymerase in cytosolic fractions prepared by a number of methods<sup>6</sup> and previous reports that suggest that up to 95% of nuclear proteins can redistribute during biochemical fractionation of cells (36). The problem of artifactual redistribution of proteins has long been investigated with respect to the steroid hormone receptors, and it required immunohistochemical evaluation of cells and tissues to resolve their location (Refs. 37–39 and references cited therein). Collectively, these results suggest that the components involved in the nuclear translocation of the AhR are functional in type II and group C cells, and they also suggest that the Arnt protein does not function in nuclear translocation mechanisms. It would appear that both the ligand-bound AhR and Arnt are required for the retention of these proteins in the nuclear compartment after subcellular fractionation but only a minor fraction of the total AhR or Arnt protein remains tightly associated with nuclear structures.

**Implications.** The amino acid sequences deduced from cDNA for the mouse AhR (23, 24) and human Arnt (19) show that both proteins contain a bHLH motif identified in proteins that bind DNA and require dimerization for function (22). Other proteins that contain bHLH motifs include E12, E47, *daughterless*, and those in the MyoD family (MyoD, myogenin, etc.). Recent data suggest that proteins that contain distinct dimerization domains can associate with each other to influence the regulation of various genes. For example, it has been reported that functional interactions can occur between MyoD and c-Jun (40), the Fos/Jun and ATF/CREB families (41), and the glucocorticoid receptor and c-Jun (42). It is intriguing to speculate that the AhR and Arnt may interact with additional proteins and that their subcellular location may influence the types of interactions that can occur. The identification of novel AhR and Arnt protein interactions may provide clues pertaining to the pleiotropic response observed in different animal species after exposure to TCDD and other halogenated aromatic hydrocarbons.

#### Acknowledgments

We thank Dr. Christopher Bradfield (Northwestern University) for many helpful discussions, critical review of the manuscript, and moral support. We also acknowledge Dr. Jonathan Jones (Northwestern University), Dr. Michael Baumann (Johns Hopkins University), and Dr. Keith Murphy (The Citadel) for helpful discussions concerning this project and Dr. Becky Prokipcak (University of Wisconsin) for review of the manuscript. We would like to thank Dawn Belt, Ed Glover, Dave Palen, and Pauline Schroeder, whose technical assistance was essential to the completion of this work. We thank Dr. Nancy Thompson (University of Wisconsin) and Dr. William Dove (University of Wisconsin) for providing monoclonal antibodies to RNA polymerase and tubulin, which were used to assess the integrity of cell fixation.

<sup>6</sup> Richard S. Pollenz, unpublished observations.

## References

- Poland, A., and J. C. Knutson. 2,3,7,8-Tetrachlorodibenzo-*p*-dioxin and related aromatic hydrocarbons: examination of the mechanism of toxicity. *Annu. Rev. Pharmacol. Toxicol.* **22**:517-554 (1982).
- Whitlock, J. P., Jr. Genetic and molecular aspects of 2,3,7,8-tetrachlorodibenzo-*p*-dioxin action. *Annu. Rev. Pharmacol. Toxicol.* **30**:251-277 (1990).
- Sutter, T. R., K. Guzman, K. M. Dold, and W. F. Greenlee. Targets for dioxin: genes for plasminogen activator inhibitor-2 and interleukin-1B. *Science (Washington D. C.)* **254**:415-418 (1991).
- Poland, A. P., and E. Glover. Variation in the molecular mass of the Ah receptor among vertebrate species and strains of rats. *Biochem. Biophys. Res. Commun.* **146**:1439-1449 (1987).
- Poland, A., E. Glover, and B. A. Taylor. The murine Ah locus: a new allele and mapping to chromosome 12. *Mol. Pharmacol.* **32**:471-478 (1987).
- Poland, A., E. Glover, and C. A. Bradfield. Characterization of polyclonal antibodies to the Ah receptor prepared by immunization with a synthetic peptide hapten. *Mol. Pharmacol.* **39**:20-26 (1990).
- Okey, A. B., G. P. Bondy, M. Mason, D. W. Nebert, C. J. Forester-Gibson, J. Muncan, and M. J. Dufresne. Temperature-dependent cytosol-to-nuclear translocation of the Ah receptor for 2,3,7,8-tetrachlorodibenzo-*p*-dioxin in continuous cell culture lines. *J. Biol. Chem.* **255**:11415-11422 (1980).
- Cuthill, S., L. Poellinger, and J.-A. Gustafsson. The receptor for 2,3,7,8-tetrachlorodibenzo-*p*-dioxin in the mouse hepatoma cell line Hepa 1c1c7. *J. Biol. Chem.* **262**:3477-3481 (1987).
- Denis, M., S. Cuthill, A.-C. Wilkstrom, L. Poellinger, and J. A. Gustafsson. Association of the dioxin receptor with the *M*, 90,000 heat shock protein. *Biochem. Biophys. Res. Commun.* **155**:801-807 (1988).
- Perdew, G. H. Association of the Ah receptor with the 90-kDa heat shock protein. *J. Biol. Chem.* **263**:13802-13805 (1988).
- Pongratz, I., G. G. F. Mason, and L. Poellinger. Dual roles of the 90-kDa heat shock protein hsp90 in modulating functional activities of the dioxin receptor. *J. Biol. Chem.* **267**:13728-13734 (1992).
- Prokipcak, R. D., and A. B. Okey. Physicochemical characterization of the nuclear form of Ah receptor from mouse hepatoma cells exposed in culture to 2,3,7,8-tetrachlorodibenzo-*p*-dioxin. *Arch. Biochem. Biophys.* **267**:811-828 (1988).
- Fujisawa-Sehara, A., K. Sogawa, M. Yamane, and Y. Fujii-Kuriyama. Characterization of xenobiotic responsive elements upstream from the drug metabolizing cytochrome P-450c gene: a similarity to glucocorticoid regulatory elements. *Nucleic Acids Res.* **15**:4179-4191 (1987).
- Denison, M., J. Fisher, and J. P. Whitlock, Jr. The DNA recognition site for the dioxin-Ah receptor complex. *J. Biol. Chem.* **263**:17221-17224 (1988).
- Hapgood, J., S. Cuthill, M. Denis, L. Poellinger, and J. A. Gustafsson. Specific protein-DNA interactions at the xenobiotic responsive element: copurification of dioxin receptor and DNA-binding activity. *Proc. Natl. Acad. Sci. USA* **86**:60-64 (1989).
- Watson, A. J., and O. Hankinson. Dioxin- and Ah receptor-dependent protein binding to xenobiotic responsive elements and G-rich DNA studied by *in vivo* footprinting. *J. Biol. Chem.* **266**:6874-6878 (1992).
- Elferink, C. J., T. A. Gasiewicz, and J. P. Whitlock, Jr. Protein-DNA interactions at a dioxin-responsive enhancer. *J. Biol. Chem.* **265**:20708-20712 (1990).
- Hoffman, E. C., H. Reyes, F. F. Chu, F. Sander, L. H. Conley, B. A. Brooks, and O. Hankinson. Cloning of a factor required for activity of the Ah (dioxin) receptor. *Science (Washington D. C.)* **252**:954-958 (1991).
- Reyes, H., S. Reisz-Porszasz, and O. Hankinson. Identification of the Ah receptor nuclear translocator protein (Arnt) as a component of the DNA binding form of the Ah receptor. *Science (Washington D. C.)* **256**:1193-1195 (1992).
- Dolwick, K. M., H. I. Swanson, and C. A. Bradfield. *In vitro* analysis of Ah receptor domains involved in ligand-activated DNA recognition. *Proc. Natl. Acad. Sci. USA* **90**:8566-8570 (1993).
- Whitelaw, M., I. Pongratz, A. Wilhelmsson, J. A. Gustafsson, and L. Poellinger. Ligand-dependent recruitment of the Arnt coregulator determines DNA recognition by the dioxin receptor. *Mol. Cell. Biol.* **13**:2504-2514 (1993).
- Jones, N. Transcriptional regulation by dimerization: two sides to an incestuous relationship. *Cell* **61**:9-11 (1990).
- Ema, M., K. Sogawa, N. Watanabe, Y. Chujoh, N. Matsushita, O. Gotoh, Y. Funae, and Y. Fujii-Kuriyama. cDNA cloning and structure of mouse putative Ah-receptor. *Biochem. Biophys. Res. Commun.* **184**:246-253 (1992).
- Burbach, K. M., A. Poland, and C. A. Bradfield. Cloning of the Ah-receptor cDNA reveals a distinctive ligand activated transcription factor. *Proc. Natl. Acad. Sci. USA* **89**:8185-8189 (1992).
- Bernhard, H. P., G. J. Darlington, and F. H. Ruddle. Expression of liver phenotypes in cultured mouse hepatoma cells: synthesis and secretion of serum albumin. *Dev. Biol.* **35**:83-96 (1973).
- Hankinson, O. Single-step selection of clones of a mouse hepatoma line deficient in aryl hydrocarbon hydroxylase. *Proc. Natl. Acad. Sci. USA* **76**:373-376 (1979).
- Legraverend, C., R. R. Hannah, H. J. Eisen, I. S. Owens, D. W. Nebert, and O. Hankinson. Regulatory gene product of the Ah locus. *J. Biol. Chem.* **257**:6402-6407 (1982).
- Miller, A. G., D. Israel, and J. P. Whitlock, Jr. Biochemical and genetic analysis of variant mouse hepatoma cells defective in the induction of benzo(a)pyrene-metabolizing enzyme activity. *J. Biol. Chem.* **258**:3523-3527 (1983).
- Whitlock, J. P., Jr., and D. R. Galeazzi. 2,3,7,8-Tetrachlorodibenzo-*p*-dioxin receptors in wild-type and variant mouse hepatoma cells. *J. Biol. Chem.* **259**:980-985 (1984).
- Harlow, E., and D. Lane. *Antibodies: A Laboratory Manual*. Cold Spring Harbor Laboratory, Cold Spring Harbor, NY (1988).
- Poland, A., E. Glover, F. H. Ebetino, and A. S. Kende. Photoaffinity labeling of the Ah receptor. *J. Biol. Chem.* **261**:6352-6365 (1986).
- Poland, A., and E. Glover. Chlorinated biphenyl induction of aryl hydrocarbon hydroxylase activity: a study of structure-activity relationships. *Mol. Pharmacol.* **13**:924-938 (1977).
- Picard, D., and K. R. Yamamoto. Two signals mediate hormone-dependent nuclear localization of the glucocorticoid receptor. *EMBO J.* **6**:3333-3340 (1987).
- Silver, P. A. How proteins enter the nucleus. *Cell* **64**:489-497 (1991).
- Pratt, W. B., L. C. Scherrer, K. A. Hutchison, and F. C. Dalman. A model of glucocorticoid receptor unfolding and stabilization by a heat shock protein complex. *J. Steroid Biochem. Mol. Biol.* **41**:223-229 (1992).
- Paine, P. L., C. F. Austerberry, L. J. Desjarlais, and S. B. Horowitz. Protein loss during nuclear isolation. *J. Cell Biol.* **97**:1240-1242 (1983).
- King, W. J., and G. L. Greene. Monoclonal antibodies localize oestrogen receptor in the nuclei of target cells. *Nature (Lond.)* **307**:745-749 (1984).
- Antakly, T., and H. J. Eisen. Immunocytochemical localization of glucocorticoid receptor in target cells. *Endocrinology* **115**:1984-1989 (1984).
- Tuohimaa, P., A. Pekki, M. Blauer, T. Joensuu, P. Vilja, and T. Ylikomi. Nuclear progesterone receptor is mainly heat shock protein 90-free *in vivo*. *Proc. Natl. Acad. Sci. USA* **90**:5848-5852 (1993).
- Bengal, E., L. Ransone, R. Scharfmann, V. J. Dwarki, S. J. Tapscott, H. Weintraub, and I. M. Verma. Functional antagonism between c-Jun and MyoD proteins: a direct physical association. *Cell* **68**:507-519 (1992).
- Hai, T., and T. Curran. Cross-family dimerization of transcription factors Fos/Jun and ATF/CREB alters DNA binding specificity. *Proc. Natl. Acad. Sci. USA* **88**:3720-3724 (1991).
- Yang-Yen, H. F., J.-C. Chambard, Y.-L. Sun, T. Smeal, T. J. Schmidt, J. Drouin, and M. Karin. Transcriptional interference between c-Jun and the glucocorticoid receptor: mutual inhibition of DNA binding due to direct protein-protein interaction. *Cell* **62**:1205-1215 (1990).

Send reprint requests to: Richard S. Pollenz, School of Pharmacy, University of Wisconsin, 425 N. Charter St., Madison, WI 53706.